

## Dopant Activation and Damage Recovery of Ion Shower Doped Poly-Si According to Various Annealing Techniques

*Jong-Hyun Park<sup>1</sup>, Dong-Min Kim<sup>1</sup>, Jae-Sang Ro<sup>1</sup>, Kyu-Hwan Choi<sup>2</sup>, and Ki-Yong Lee<sup>2</sup>*

<sup>1</sup>Dep't of Mat. Sci. and Eng., Hongik University, Seoul, Korea 82-2-320-1698 jsang@wow.hongik.ac.kr

<sup>2</sup>Samsung SDI CO., LTD., Gyeonggi-do, Korea

### Abstract

*Source/drain (or, LDD) formation technology is critical to device reliability especially in the case of short channel LTPS-TFT devices. Ion shower doping with a main ion source of  $P_2H_x$  was conducted on ELA Poly-Si. We report the effects of annealing methods on dopant activation and damage recovery in ion-shower doped poly-Si.*

### 1. Introduction

Non-mass analyzed ion shower doping technique has been widely used for source/drain doping, for LDD (lightly-doped-drain) formation, and for channel doping in fabrication of low-temperature poly-Si thin-film transistors (LTPS-TFT's) [1,2]. Dopant activation may be done by FA (furnace annealing), RTA (rapid thermal annealing), and ELA (excimer laser annealing), respectively [3]. When we are dealing with annealing methods we should consider both the electrical activation of implanted impurities and the annealing primary crystalline defects.

As the channel length becomes short, device reliability of LTPS-TFT's should be seriously taken into account [4]. There are many factors affecting the reliability of TFT devices. We believe that damage recovery by activation annealing plays an important role among them. Here, we report the effects of annealing methods on dopant activation and damage recovery.

### 2. Experimental

The substrates used were poly-Si produced by excimer laser crystallization on 500 Å-thick PECVD (plasma enhanced chemical

vapor deposition) a-Si. Phosphorous was implanted by ion shower doping with a main ion source of  $P_2H_x$  using a source gas of  $PH_3/H_2$  [5]. Acceleration voltage was changed from 1 kV to 15 kV and doping time varied from 10 sec to 3 min. as variables of implantation conditions. Activation annealing was performed by FA, and ELA, respectively. The sheet resistance was measured using a 4-point-probe and the crystallinity was determined by UV-transmittance.

### 3. Results and discussion

Fig. 1 shows the defect density calculated by TRIM-code simulation as a function of acceleration voltage. The defect density was obtained by integrating primary-defect concentration from 0 Å to 500 Å assuming a dose of  $1 \times 10^{15} \text{cm}^{-2}$ . The amount of as-implanted damage induced in 500 Å-thick poly-Si films is seen to increase with an acceleration voltage. This trend is consistent with the results obtained by UV-transmittance as shown in Fig. 2. Measured crystallinity decreases with acceleration voltage and doping time. Crystallinity drops rapidly with the acceleration voltage in the range of 1 kV to 5 kV, and then more gradually beyond 5 kV. The calculated defect density has a similar relationship with acceleration voltage as implied in Fig. 1. Crystallinity for ELA poly-Si was measured to be ~0.8, while that for the 15 kV-implanted sample at a doping time of 3 min approaches almost to the level of amorphous silicon.

When we annealed the samples implanted with a doping time of 1 min in the range of 550°C to 650°C for 30 min, the sheet

resistance was observed to decrease with an acceleration voltage. The sheet resistance was measured to be below the level of  $1,000 \Omega/\square$  for the samples implanted with acceleration voltages exceeding 5 kV irregardless of the above annealing conditions. Fig. 3 shows the sheet resistance as a function of acceleration voltage for the samples implanted with a doping time of 3 min. The sheet resistance decreases with the increase in acceleration voltage in the range of 1 kV to 10 kV. It, however, increases for the 15 kV- implanted sample following FA-treatments in the range of  $550^{\circ}\text{C}$  to  $600^{\circ}\text{C}$  for 30 min, as indicated in Fig. 3. The sheet resistance does not, however, rise for the sample annealed at  $650^{\circ}\text{C}$  for 30 min as demonstrated in Fig. 3.

Since the implantation condition with the acceleration voltage of 15 kV induces more damage than any other conditions involved in this study we changed the doping time and annealing conditions using the samples implanted with this energy in order to investigate the characteristics of dopant activation and damage recovery. Fig. 4 shows the sheet resistance as a function of doping time for the FA-treated samples at  $550^{\circ}\text{C}$  (triangles),  $600^{\circ}\text{C}$  (circles), and  $650^{\circ}\text{C}$  (squares), respectively for 30 min, following ion shower doping with the acceleration voltage of 15 kV. The sheet resistance reaches the value below  $1,000 \Omega/\square$  within the doping time of 1 min. Furnace annealing for 30 min in the range of  $550^{\circ}\text{C}$  to  $650^{\circ}\text{C}$  resulted in almost the same efficiency of dopant activation within the doping time of 1 min. The sheet resistance decreases and saturates within in this period of doping time, Regime I, Dose- Controlled-Regime as illustrated in Fig. 4. The sheet resistance, however, increases beyond the doping time of 1 min except for the case of  $650^{\circ}\text{C}$ -30 min FA-treatments. Rise in the sheet resistance for the samples implanted

with a high dose was found to be due to uncured damage as implied in Fig. 5. Crystallinity measured by UV-transmittance for the as-implanted samples with various doping time was observed to have value below  $\sim 0.15$ , while that for ELA poly-Si,  $\sim 0.8$ , as indicated in Fig. 5. Crystallinity for the samples implanted for 2 min and 3 min was measured to be in the level of below  $\sim 0.2$  even after FA-treatments at  $600^{\circ}\text{C}$ , while that for 10 sec and 20 sec reaches to the value of  $\sim 0.8$ . This observation clearly demonstrates that uncured damage is responsible for the rise of sheet resistance for the samples implanted with a heavy dose (Regime II : Damage-Controlled-Regime as illustrated in Fig. 4). Although the sheet resistance dose not rise at a doping time beyond 2 min for the samples annealed at  $650^{\circ}\text{C}$  for 30 min, damage is not sufficiently recovered as implied in Fig. 5. Damage-recovery proceeds gradually with the annealing temperature and time, while the kinetics of dopant activation was observed to be a relatively rapid process.

We performed excimer laser annealing using the samples implanted with the same acceleration voltage of 15 kV in order to compare the results obtained by FA-treatments. We chose  $200 \text{ mJ}/\text{cm}^2$  as a laser energy density, the condition of partial melting in  $500 \text{ \AA}$ -thick poly-Si films. Fig. 6 indicates the sheet resistance as a function of doping time for the 15 kV-implanted samples after ELA-treatments at an energy density of  $200 \text{ mJ}/\text{cm}^2$ . The sheet resistance is below the level of  $1,000 \Omega/\square$  for all samples involved. It decreases with a doping time within 2 min, but increases beyond 2 min. The change of the sheet resistance as a function of doping time is shown to have similar trend with that of the FA-treated samples. Damage, however, is not easily recovered by  $200 \text{ mJ}/\text{cm}^2$ -ELA treatments, as illustrated in Fig. 7, in

contrast to the results of FA-treatments. Crystallinity for the ELA-treated samples at this condition lies in the value of  $\sim 0.4 - \sim 0.5$  within a doping time of 2 min, and below the level of  $\sim 0.3$  at a doping time of 3 min.

#### 4. Conclusions

To summarize, damage recovery is rather a slow process, while the kinetics of dopant activation is relatively rapid. Damage-recovery should be considered seriously in addition to dopant activation when we choose the means of activation-annealing. Annealing techniques with sufficient thermal-budget may be required for curing damage efficiently.

#### 5. Acknowledgements

This research was supported by a grant (M1-02-KR-01-0001-02-K18-01-012-11) from Information Display R&D Center, one of the 21st Century Frontier R&D Program funded by the Ministry of Science and Technology of Korean government.

#### 6. References

- <sup>1</sup> Yasuyoshi Mishima and Michiko Takei, J. Appl. Phys. **75** (10), 4933 (1994)
- <sup>2</sup> G. Kawachi, T. Aoyama, K. Miyato, Y. Ohno, A. Mimura, N. Komishi, and Y. Mochizuki, J. Electrochem. Soc. **137** (11) 3522 (1990)
- <sup>3</sup> G. Kawachi, T. Aoyama, Akio Mimura, and N. Konishi, Jpn. J. Appl. Phys. **33** 2092 (1994)
- <sup>4</sup> L. Mariucci, G. Fortunato, R. Carluccio, A. Pecora, S. Giovannini, F. massussi, L. Colalongo, and M. Valdinoci, J. Appl. Phys. **84**, 2341 (1998)
- <sup>5</sup> K. Chen, G.J. Ra, Y. Shao, G. Mo, S. Lichtenthal, and J. Blake, Proceedings of 1998 International Conference on Ion Implantation Technology, 1218 (1998)

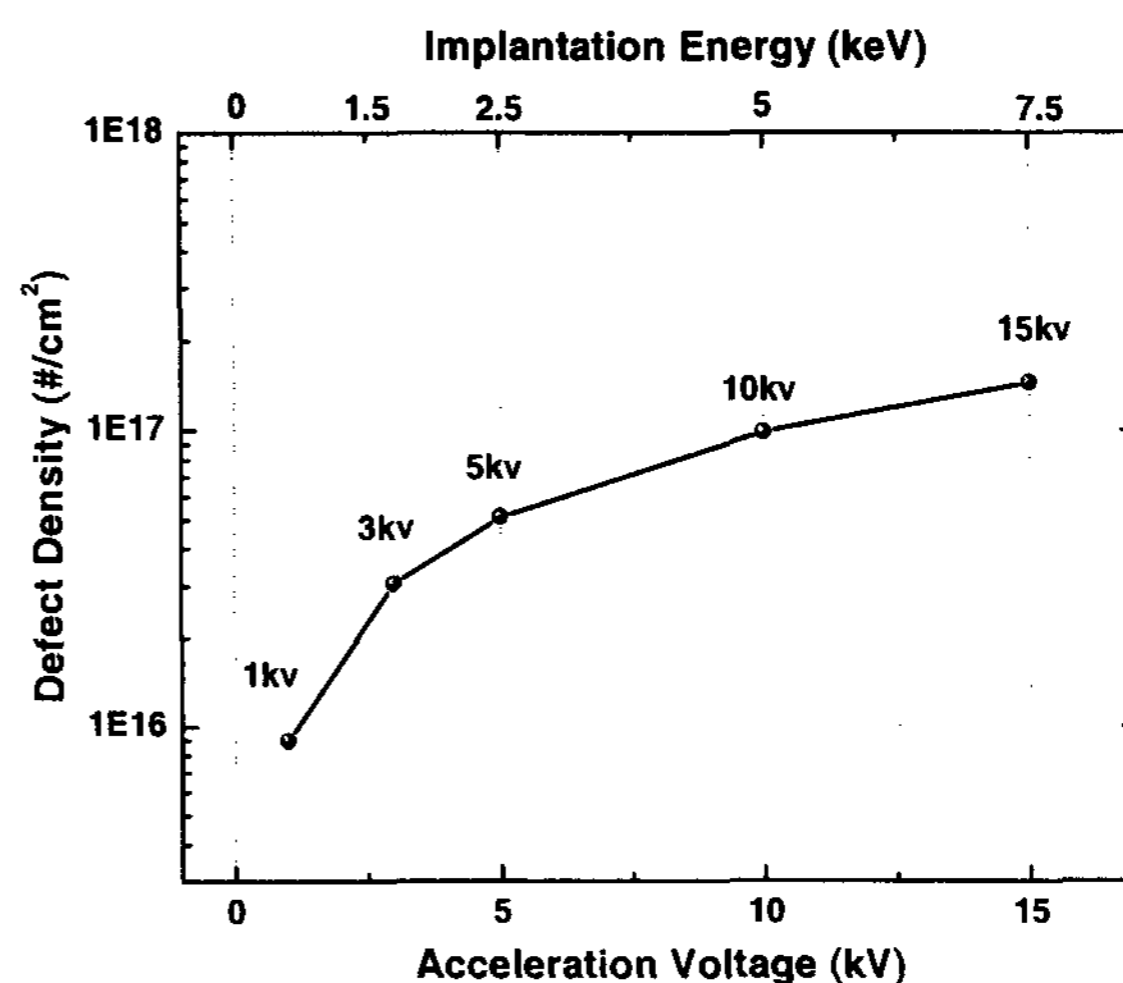


Fig. 1 Calculated defect density as a function of acceleration voltage using TRIM-code simulation. The defect density (#/cm<sup>2</sup>) was calculated by integrating primary-damage profile from 0 to 500 Å.

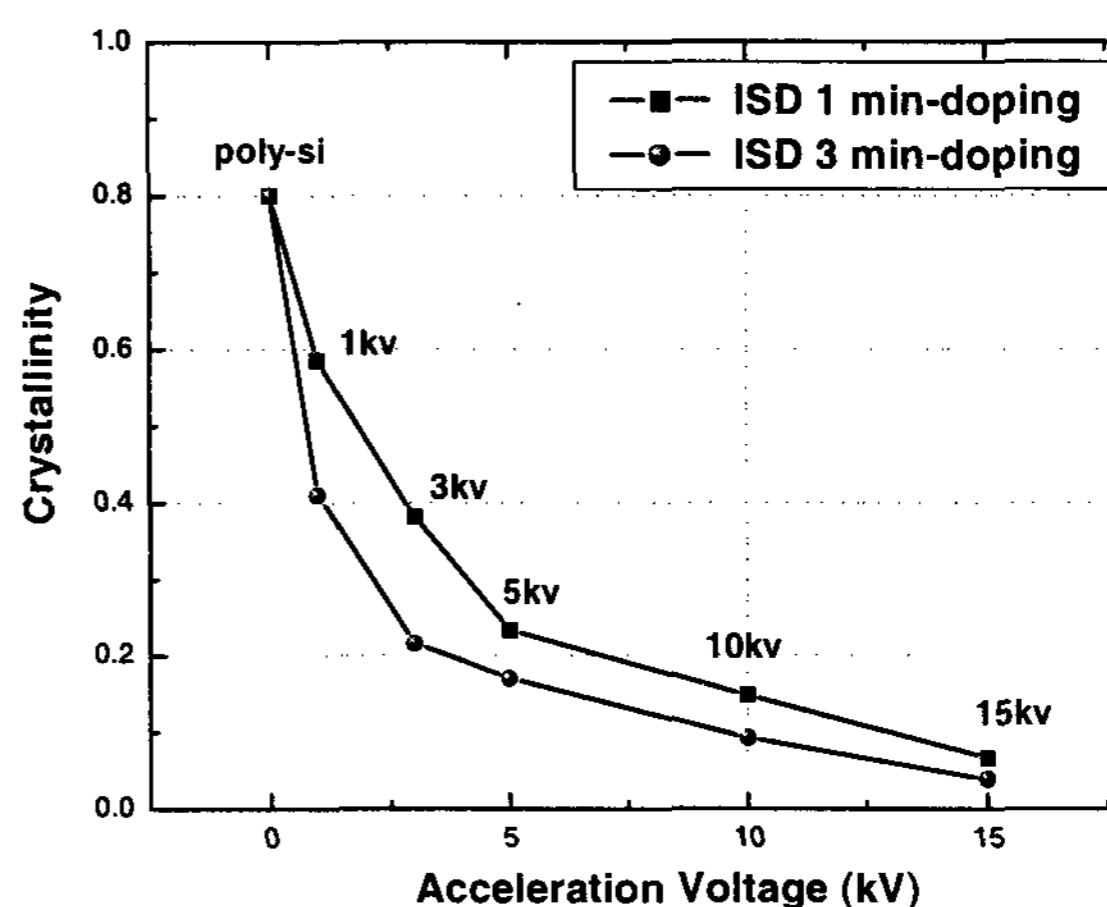


Fig. 2 Measured crystallinity vs. acceleration voltage using UV-transmittance.

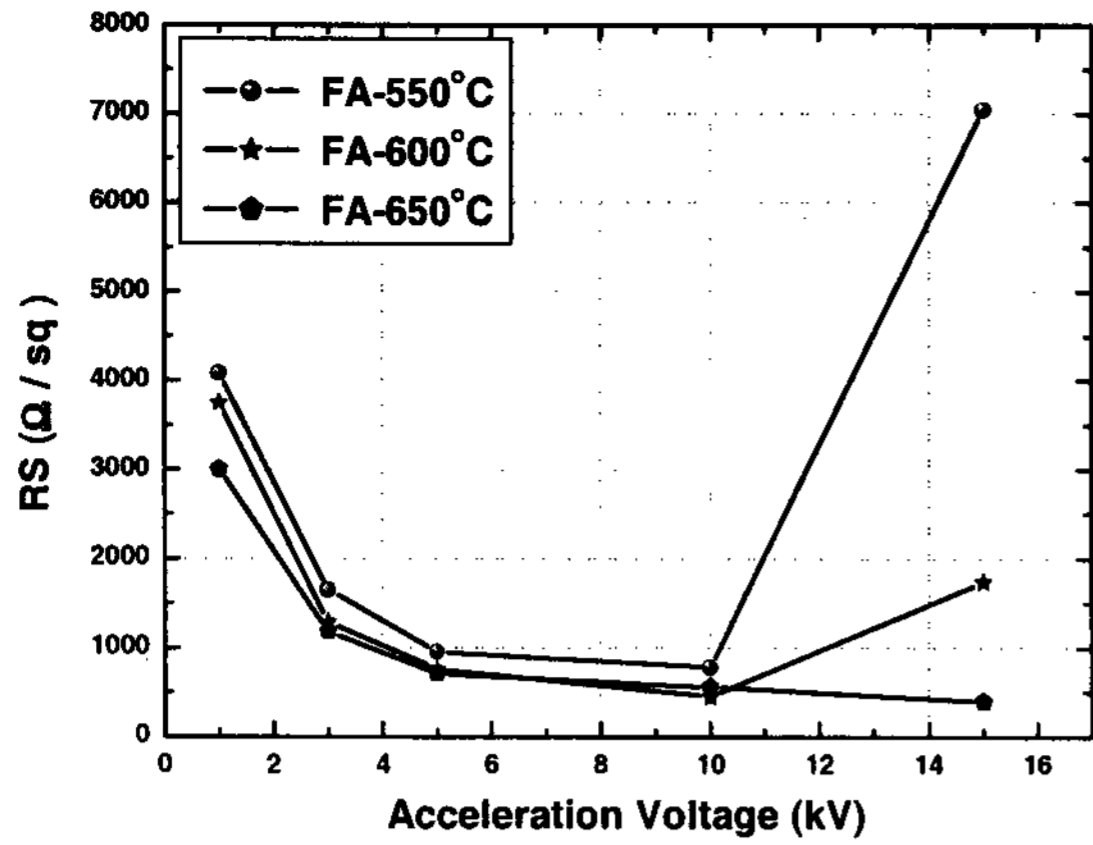


Fig. 3 Sheet resistance vs. acceleration voltage for the samples annealed for 30 min at 550°C, 600°C and 650°C, respectively.

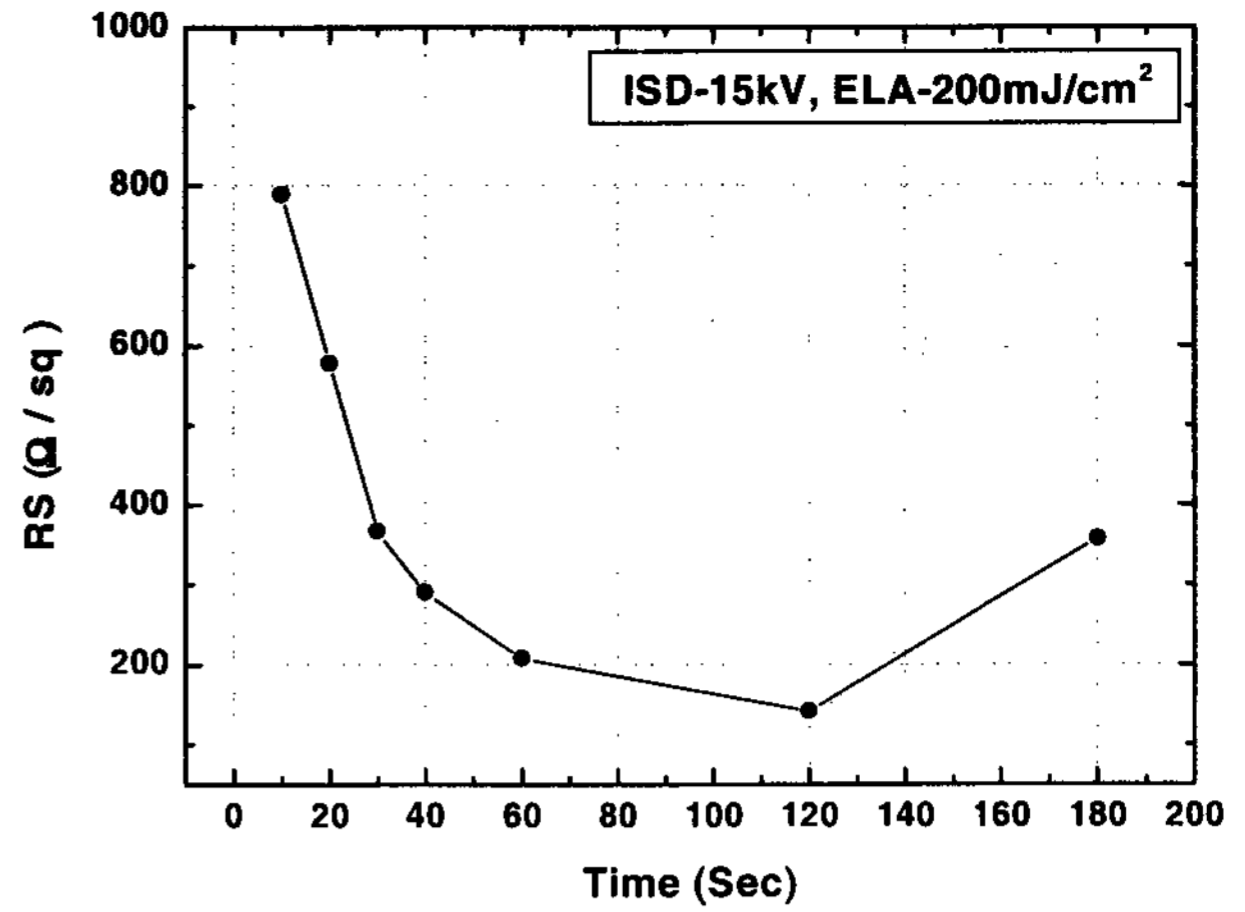


Fig. 6 Sheet resistance vs. doping time for the 15 kV-implanted samples, annealed at an excimer laser energy density of 200 mJ/cm²

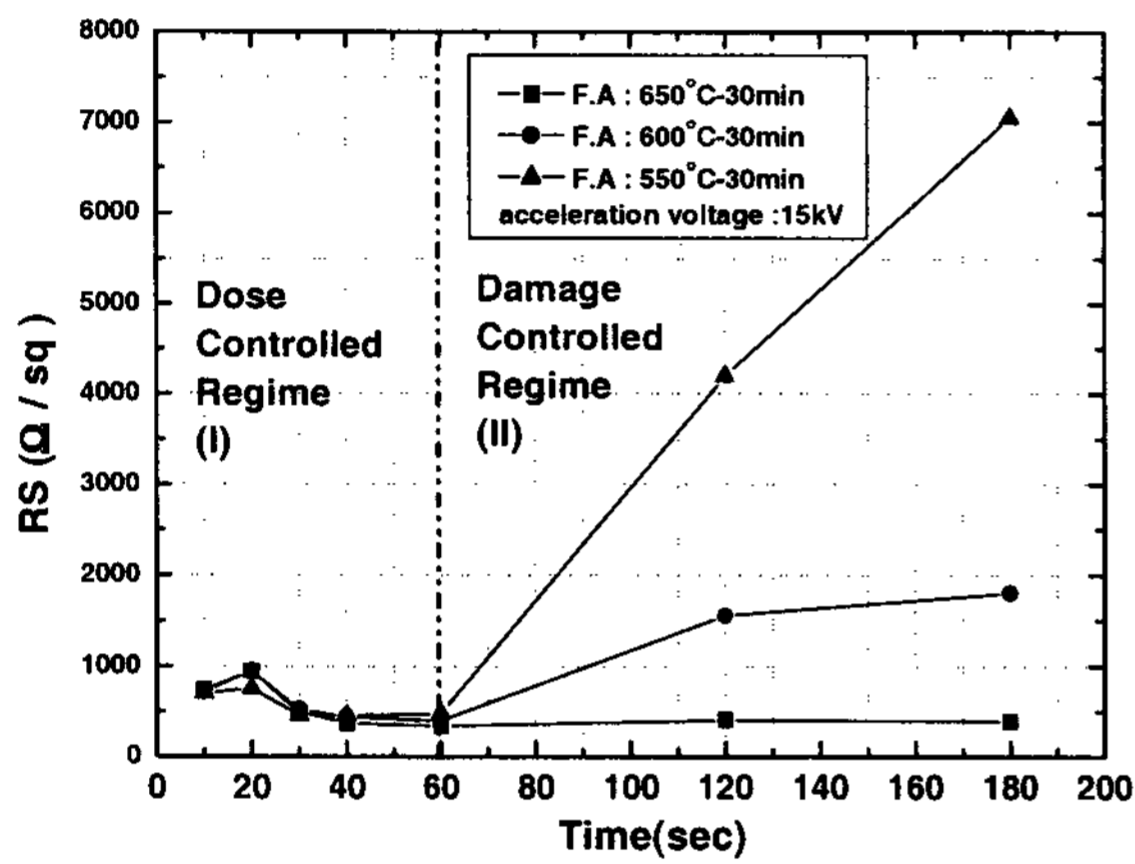


Fig. 4 Sheet resistance vs. doping time for the samples annealed at 550°C (triangles), 600°C (circles), and 650°C (squares), respectively.

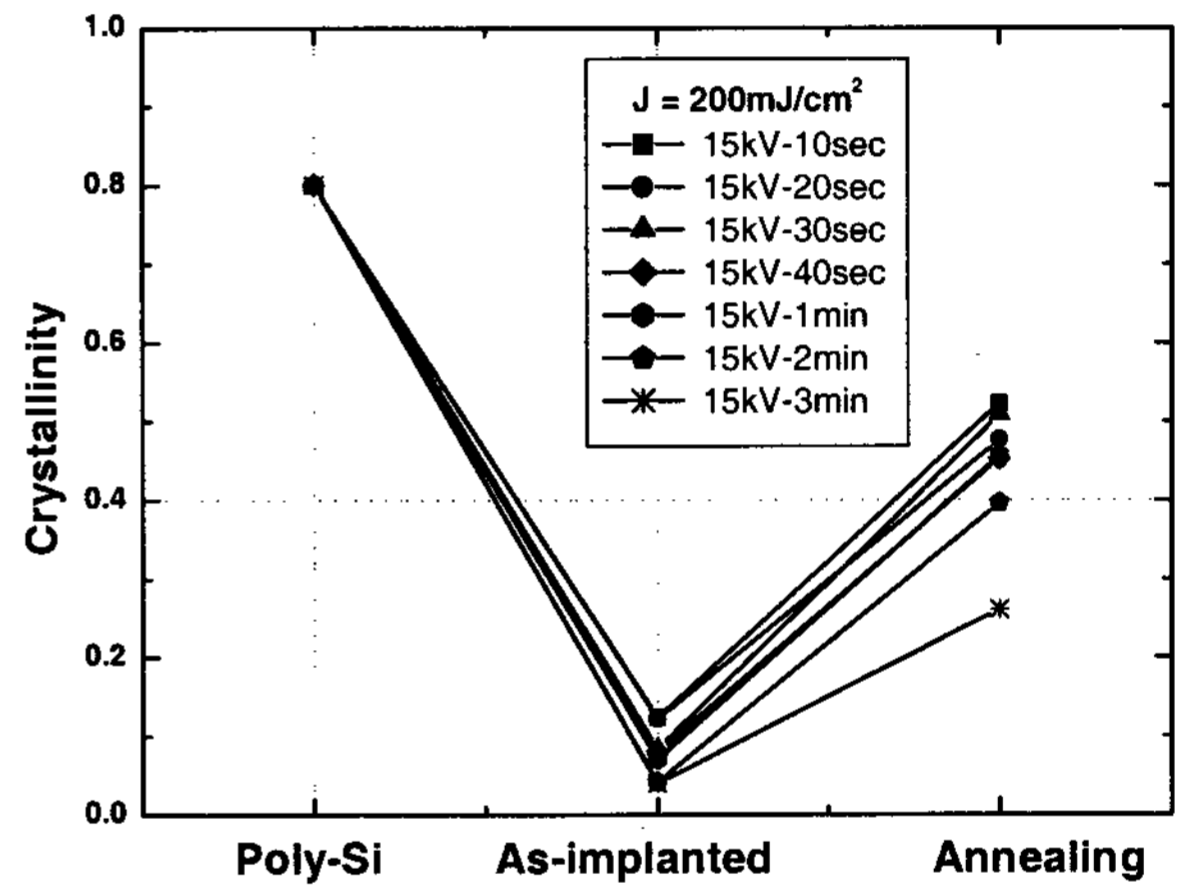


Fig. 7 Measured crystallinity for Laser-poly-Si, as-implanted samples and as-ELA-treated samples, respectively

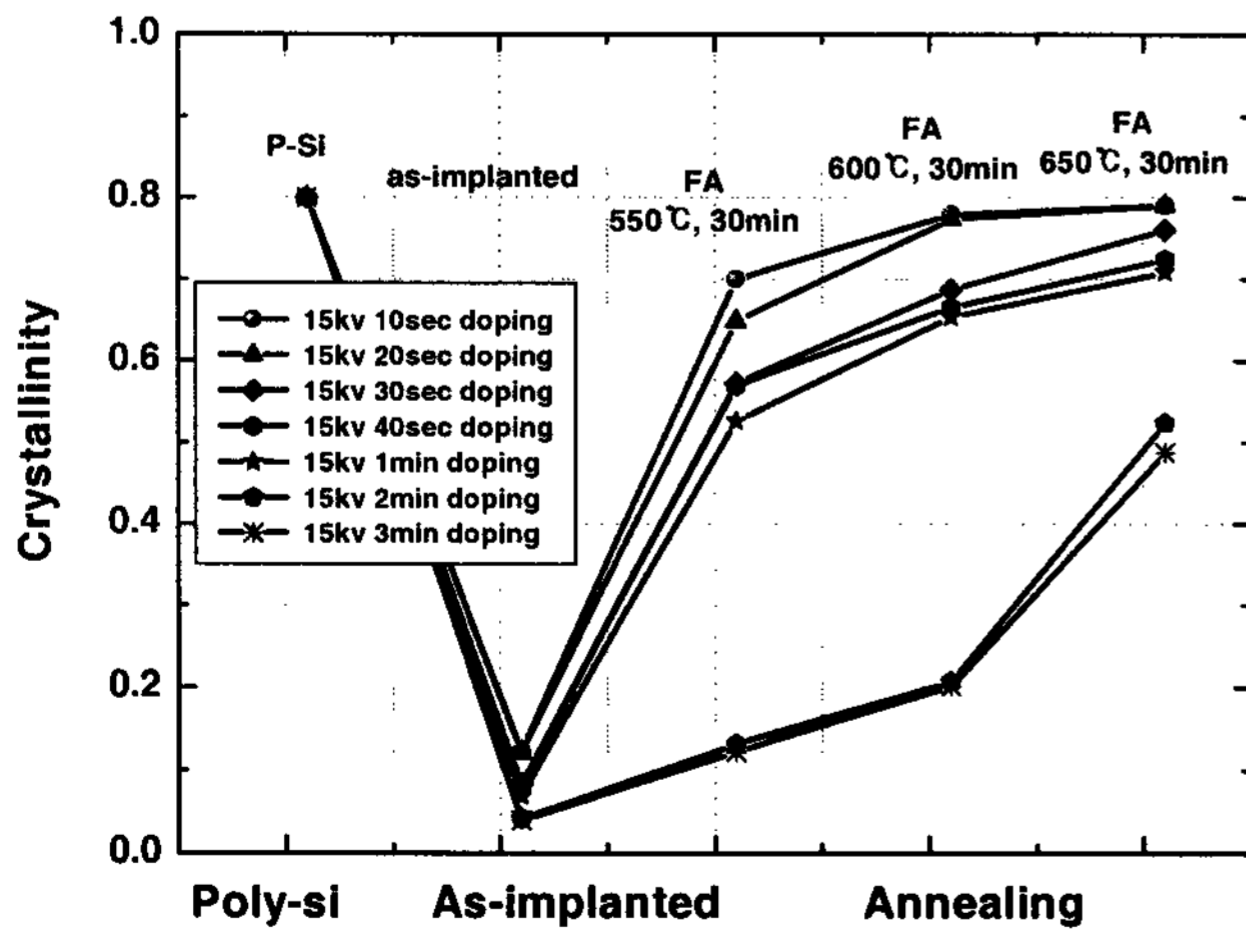


Fig. 5 Measured crystallinity for Laser-poly-Si, as-implanted samples and as-FA-treated samples, respectively